

RESERVE THIS SPACE

Metrology as a Tool to Understand Immobilized Enzyme Catalyzed Ring-Opening Polymerization.

Matthew T. Hunley, Sara V. Orski, and Kathryn L. Beers*

**Materials Science and Engineering Division, National Institute of
Standards and Technology, Gaithersburg, MD 20899, United States**

**Present address: National Institute of Standards and Technology,
100 Bureau Drive, MS 8542, Gaithersburg, MD 20899**

***Email: beers@nist.gov**

Enzyme-catalyzed polymerization provides a green alternative to synthesize biodegradable polyesters over conventional heavy metal catalysts. Heterogeneous catalysis, where the enzyme is immobilized onto solid-supports, allows for easy catalyst removal and can increase the commercial feasibility of biocatalysis with a thorough understanding of the reaction kinetics and required process conditions. In this mini-review, we describe our comprehensive metrology approach to fully identify key parameters to control enzymatic ring-opening polymerization (ROP) of lactones: development of predictive models of reaction kinetics, experimental models of the catalyst surface micro-environment, and on-line spectroscopic analysis of reaction conversion for polyester homopolymers and copolymers. Quantitative evaluation of enzymatic ROP elucidates advantages and limitations of current enzyme-catalyzed polymerizations and aids in the design of

RESERVE THIS SPACE

better reaction conditions and next generation catalysts.

Introduction

Awareness of sustainability and polymer lifecycle analysis has driven the development of many novel as well as commercial monomers from renewable feedstocks. Many commercially-important bioderivable, degradable polymers, including poly(lactic acid (PLA) and polycaprolactone (PCL), are synthesized via ring-opening polymerization (ROP) using organometallic catalysts. Conventionally, this class of polymers is synthesized in bulk using $\text{Sn}(\text{Oct})_2$ as the catalyst for controlled molecular masses and low polydispersities. However, the heavy metal catalyst often remains in the polymer and can pose a risk of toxicity. Recent interest in ROP using enzyme catalysts and organocatalysts^{1,2} suggests that the the same polymers can be controllably synthesized without the presence of toxic metals.

Many different enzymatic catalysts have been identified for the ROP of lactones, cyclic carbonates, and lactides, as well as the polycondensation of carboxylic acids with alcohols.³⁻⁵ Lipase enzymes traditionally serve as degradation catalysts by cleaving ester linkages into carboxylic acids and alcohols in nature. These same catalysts can be induced to promote polymerization by stressing them in the presence of high concentrations of monomer in organic media. Previous studies have shown that many lipases are highly active under milder conditions than conventional metal catalysts, and the enzyme structure can dictate enhanced selectivity of stereochemistry and polymer structure. Enzymes can also be readily immobilized onto solid supports for heterogeneous catalysts with little loss of activity. One popular commercialized heterogenous enzyme catalyst is *Candida antarctica* Lipase B (CAL B) immobilized on an acrylic resin. Such heterogeneous catalysts can help in achieving proper stoichiometry and allow facile catalyst removal after the reaction. For these reasons, lipase enzymes have received significant interest as “green chemistry” alternatives for heavy metal catalysts.

The commercial adoption of enzymatic catalysts, however, requires a thorough understanding of the kinetic pathways and the catalyst stability. Previous studies have indicated that water content has a tremendous impact on initiation, polymerization kinetics, cyclic formation, polymer molecular mass, and enzyme activity over time. Similarly, copolymerization studies have demonstrated mutual reactivities of a wide range of monomers via the formation of statistical copolymers. These studies have not resulted in a complete framework to fully understand enzyme catalyzed polymerizations. We have approached enzyme catalysis with the objective of enhanced understanding

through improved measurement techniques and predictive models. In this mini-review, we focus on the results of our recent work to understand the stability of solid-supported CAL B enzyme, develop a predictive model of polymerization, and improve the metrology through polymerization monitoring and reactor design.

Evaluating Enzyme Catalyst Surface Stability

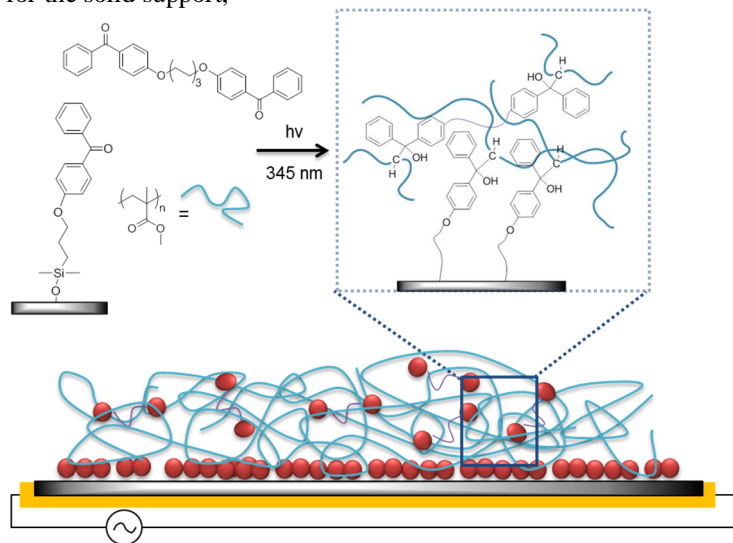
Heterogeneous catalysts allow for the easy removal and recovery of the catalyst from the reaction mixture for potential reuse in subsequent polymerizations. Catalyst recycling is an important factor in increasing commercial acceptance of CAL B-catalyzed ring-opening polymerizations, as the catalyst must have a high polymer yield to offset the increased production costs associated with enzymes⁶ over current metallic catalysts.

CAL B catalyzed ROP of ϵ -CL yields PCL with high molecular weights, and conversion rates based on choice of reaction solvent, temperature, and trace water content.^{7,8} Decreasing reaction rates over multiple cycles, often indicates enzyme desorption, which limits recyclability and contaminates the PCL product.^{9,10} This leaching is frequently attributed to the weak hydrophobic interactions of the enzyme physisorbed at the acrylic resin surface. Quantitative measurement of enzyme desorption to confirm that theory is challenging, however, as concentrations of leached enzyme within the polyester are exceedingly low.⁹ Attempts to measure enzyme leaching have been evaluated indirectly through monitoring monomer conversion over several reuse cycles⁹ or by elemental analysis of the acrylic resin.¹⁰ Furthermore, isolating potential causes of catalyst leaching is challenging due to the complex structure of the immobilized catalyst on the surface of a crosslinked, porous, polymer bead. A more direct method is needed to understand the physiochemical interaction between the enzyme and the crosslinked poly(methyl methacrylate) (PMMA) surface, so that optimal process conditions can be used to maintain adequate polymerization control and improve catalyst retention for several reuses.

Quartz crystal microbalance with dissipation monitoring (QCM-D) has been used to characterize in situ enzyme and protein adsorption at surfaces,¹¹⁻¹³ including CAL B adsorption on self-assembled monolayers.¹⁴⁻¹⁶ Mass adsorbed on a quartz crystal sensor will cause small changes in resonant frequency (f) and energy dissipation (D) of the oscillating sensor.¹⁷ These changes can be used to determine mass and viscoelastic properties of an adsorbed layer through Kelvin-Voigt viscoelastic models.¹⁸

The microenvironment of the PMMA bead surface was mimicked by fabrication of a homogenous, highly crosslinked PMMA thin film on a QCM-D sensor. The PMMA chains were covalently crosslinked to the quartz sensor

using a photoactivated benzophenone moiety within the polymer thin film and as a self-assembled monolayer on the crystal surface, as depicted in Scheme 1. The dual photochemical process permits efficient covalent attachment of commercially available PMMA to the surface and to other neighboring chains. The flat, 2D PMMA layer replaces the chemistry and mechanical properties of the bead surface in QCM-D, where enzyme adsorption, desorption, and changes in viscoelastic properties could be measured in situ as experimental conditions were varied. Enzyme stability was evaluated with increasing water content of toluene and polycaprolactone solutions, and with increasing reactor temperature, mimicking reaction environments where enzyme leaching and changing enzymatic activity has been previously demonstrated. The 2D experimental model was used to quantitatively study the enzyme stability at the polymer surface microenvironment, pinpointing the sources of variation in enzyme affinity for the solid support,



Scheme 1. Depiction of two-dimensional crosslinked PMMA thin film on quartz crystal sensor (side view). Reproduced with permission from reference 19. Copyright 2013 The American Chemical Society.

Adsorption of CAL B on the PMMA surface occurred rapidly in the QCM-D cell, as 90 % of the enzyme adsorption was complete within 300 s of addition to the QCM-D under flow, resulting in a mass surface coverage of $530 \text{ ng/cm}^2 \pm 63 \text{ ng/cm}^2$, determined by the Sauerbrey equation (equation 1).¹⁹ All Sauerbrey masses calculated represent one standard deviation among at least three trials. The overtone is denoted by n and C is a constant dependent on crystal properties, which is $17.7 \text{ ng cm}^{-2}\text{Hz}^{-1}$.

$$\Delta m = -\frac{C}{n} \Delta f_n \quad (1)$$

Generally, if the ratio of dissipation to frequency, $\Delta D_n/(-\Delta f_n/n)$, is less than 4×10^{-7} ,²⁰ the layer on the sensor can be approximated as rigid, which is true for the adsorption of CAL B on crosslinked PMMA.

Enzyme surface stability was first evaluated as a function of increasing the trace water content in reaction solvent (toluene) from 250 ppm to 450 ppm. This range was used to evaluate CAL B at a model surface over a range where the enzyme surface transitions from dehydrated and inactive (≤ 250 ppm) to fully hydrated (≥ 450 ppm) during ϵ -CL ROP conditions.⁹ Sauerbrey calculations yielded an 8 % decrease in mass surface coverage of the enzyme at 350 ppm and a 20.2 % decrease at 450 ppm among several trials.¹⁹ PMMA control samples demonstrated an insignificant mass increase at 450 ppm, due to water adsorption on the PMMA layer. The CAL B desorption from the surface is caused by the disruption of the hydrophobic interaction between the enzyme and the PMMA surface, as the enzyme absorbs water and becomes less rigid.

Formation of the enzyme-activated complex (EAC) was evaluated by measuring adsorption of polycaprolactone ($M_n = 10,000$ g/mol) to CAL B active sites with increasing water content (250 ppm – 450 ppm). Mass adsorption changes due exclusively to the EAC were evaluated as the difference between enzyme-modified and unmodified PMMA, deconvoluting the mass change of the EAC from non-specific binding of PCL to the surface. The measured increase in mass of the EAC with additional water content was inconsistent with the enzyme loss observed with increasing water concentration in toluene. This difference results from the influence of water on polymerization kinetics,²¹ where the concentration of free polyester chains in solution over those bound to the enzyme increases as trace water content increases. This creates increased diffusion of PCL chains to active enzymes and the water affinity between the enzyme and PCL will retain greater mass at the sensor surface.

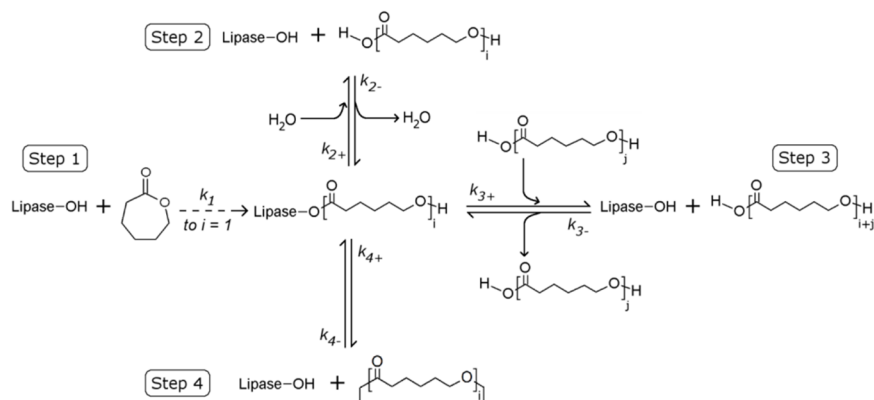
The PMMA/CAL B interfacial stability was also evaluated as a function of temperature between 22 °C and 90 °C. Bare crystal and PMMA control samples were measured under identical conditions to determine the response of the CAL B layer corrected for background effects such as temperature dependence on frequency and dissipation of the quartz crystal, as well as the temperature effects on solvent density and viscosity. Mass surface coverage of the CAL B layer decreases with increasing temperature; 90% of the enzyme layer is desorbed at 90 °C.¹⁹ The frequency and dissipation changes of the CAL B/PMMA and PMMA layers indicate that the enzyme layer becomes more viscoelastic as temperature increases. The ratio of $\Delta D_n/(-\Delta f_n/n)$ for CAL B is right at the approximation threshold, where the film can be approximated as rigid below 50 °C, and viscoelastic above. The CAL B layer therefore remains mostly elastic, with minimal diffusion and relaxation occurring between the surface-bound enzymes. Increasing temperature disrupts the CAL B layer, permitting

enzyme diffusion from the PMMA surface, which is reversible upon cooling. Mass loss due to enzyme dehydration will be minimal, however, since only water adsorbed at the enzyme surface can be removed by organic solvents.²²

The development of a simplified 2D experimental model of the CAL B/polymer interface has demonstrated the chemical affinity of CAL B for PMMA on a flat, smooth surface with varying reaction parameters. This model establishes a reproducible in situ model, which may be used to expand enzyme affinity measurements to include more complex interactions induced by a porous particle geometry of the heterogeneous catalyst bead.

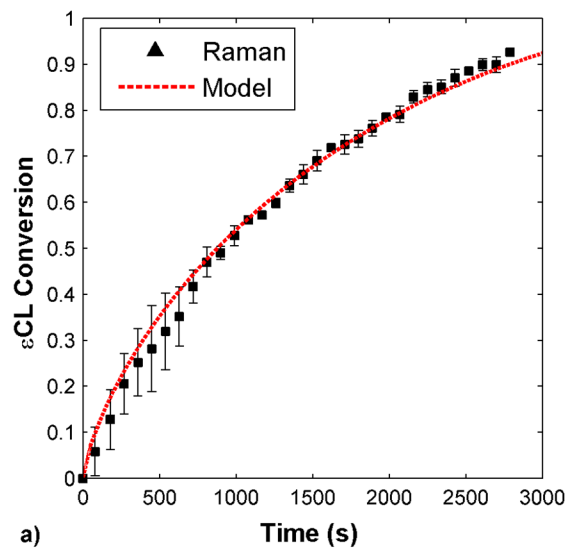
Understanding the Kinetic Pathways

Enzyme-catalyzed ring-opening polymerization (ROP) proceeds via several distinct steps which all require the presence of lipase.^{8,21} Scheme 2 illustrates the central role of lipase catalyst in the ROP mechanism of ϵ -caprolactone (ϵ -CL).²¹ The active site reacts to open the monomer ring to form the enzyme-activated monomer (EAM) (Step 1 in Scheme 2). The EAM can then react with water to form ring-opened monomer (Step 2), a propagating polymer chain to form polymer (Step 3), or intramolecularly to form cyclics (Step 4). The lipase also reacts with oligomeric and polymeric species to drive these reactions in reverse.

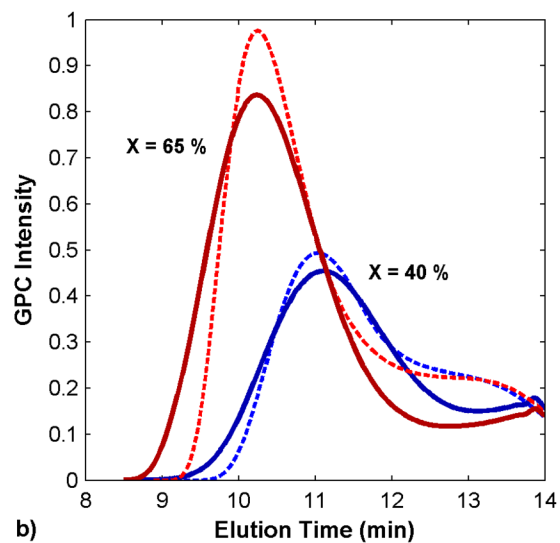


Scheme 2. Kinetic Reactions in the Enzyme-Catalyzed Polymerization of ϵ -Caprolactone. Reproduced with permission from reference 21. Copyright 2012 The American Chemical Society.

Earlier studies demonstrated the influence of water on initiation and the prevalence of cyclics within the polymer product.²³⁻²⁵ However, these early reports had no predictive capabilities. We adopted the generally accepted mechanism⁸ into a robust kinetic model to track the evolution of all species (including ring-opened monomer, cyclics, and all polymer chains) over the course of polymerization. The results of the kinetic model simulation of ϵ -CL polymerization using CAL B enzyme are shown in Figure 1. The model monomer conversion mirrored the experimentally observed monomer conversion to within measurement error, but more impressively the model molar mass distribution showed very similar behavior to the experimental SEC traces. The tailing at high elution times demonstrates the presence of low molar mass cyclic oligomers, even at high monomer conversions. These low molar mass species act as plasticizers with detrimental effects on polymer physical properties.



a)



b)

Figure 1. (a) Comparison of experimental (■) and model(---) results for ϵ -CL ring-opening conversion. (b) Experimental (---) and modeled (—) SEC traces for molecular mass distribution at 40 % (blue) and 65 % (red) conversion. Reproduced with permission from reference 21. Copyright 2012 The American Chemical Society.

Another major factor in the enzyme-mediated ROP revealed by the kinetic model is the influence of water, which affects all stages of polymerization from initiation to degradation. The model indicated that the ring-opening reaction proceeded faster with higher water concentrations. Because water affects the release of enzyme-activated monomer (EAM) from the enzyme active sites, lower water concentrations lead to longer residence times of EAM, slowing the overall polymerization rate. Further experiments confirmed the influence of water on M_n . Since each water molecule acts as an initiator, reduction in the water concentration should reduce the number of chains and result in increased M_n at equivalent monomer conversions. Water concentration was controlled rudimentarily through the addition of molecular sieves to the polymerization mixture. The molecular sieves slowly remove water from the reaction mixture, resulting in little change in reaction kinetics during most of the reaction but an increase in M_n at high conversions. Experimental results confirmed the model predictions, demonstrating that the molecular sieves led to a dramatic increase in M_n at high conversion.²⁶

Similarly, the kinetic model provided insight into the enzymatic degradation of polymers. When the starting material is switched from ϵ -CL to PCL, chain equilibrium reactions dominate.²¹ At long times, the PCL will reach a new equilibrium molecular mass determined by the starting M_n and the amount of additional water present. If the amount of water present is less than the number of polymer chains, then the degradation will first result in a bimodal molecular mass distribution as a portion of the polymer is degraded to lower molar mass. Afterwards, the enzyme will equilibrate all the chains to a molecular mass consistent for the number of linear chains. This equilibrium molecular mass is slightly higher than the mass of the initially degraded chains. This model behavior was confirmed experimentally.

Reaction Monitoring

In addition to the predictive capabilities of the model for enzyme kinetics, on-line reaction monitoring provides a wealth of knowledge about the polymerization. Off-line analytical techniques can be time consuming and labor intensive, and removal and storage of reaction aliquots is difficult for moisture-sensitive reactions such as enzyme-mediated ROP. Enzyme leaching can also contaminate the aliquots and lead to residual polymerization prior to analysis. On-line spectroscopic monitoring via Raman or infrared spectroscopy reduces these concerns and can provide rapid data collection over the entire reaction time.

Raman spectroscopy was used to follow the consumption of ϵ -CL by monitoring the monomer's anti-symmetric ring stretching absorbance at

696 cm^{-1} .²⁷ Figure 2 shows the monomer conversions versus reaction time for the enzyme-catalyzed ROP at different temperatures. The spectroscopic data was confirmed by ^1H NMR aliquots taken at specific time intervals, indicating that the consumption of monomer reflected incorporation into the polymer and not just ring-opening. In addition, the spectroscopic method enables a higher data density during the reaction; data collection from reaction aliquots is intrinsically limited to maintain reaction stoichiometry. The conversion data in Figure 2 also indicate that increasing temperature does not have a linear effect on the reaction kinetics. Above 55 °C, increasing the temperature leads to only a minute increase in reaction rate, possibly due to slight denaturation of the enzyme.

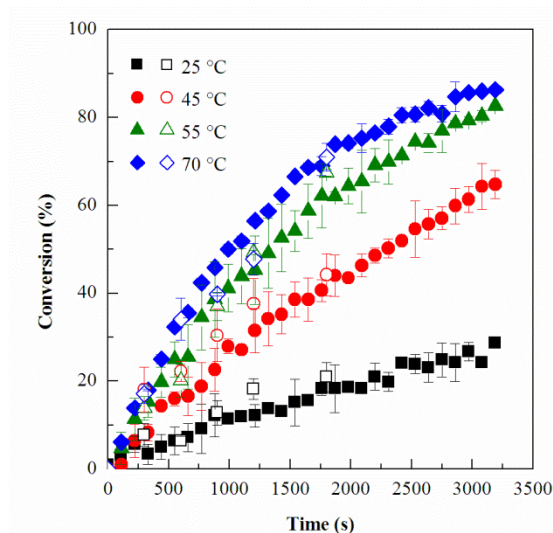


Figure 2. Conversion of ϵ -CL as a function of reaction times at different temperatures: (■)25 °C, (●)45 °C, (▲)55 °C, (◆)70 °C. Open symbols represent NMR data collected off-line, closed symbols represent Raman spectroscopic data. Reproduced with permission from reference 27. Copyright 2012 The Royal Society of Chemistry.

On-line spectroscopic analysis also enables the simultaneous monitoring of multiple monomers during copolymerizations and provides many more data points in the low conversion regime to decrease measurement uncertainty when calculating reactivity ratios. The properties of copolymers are strongly influenced by the relative reactivities and sequence distributions of different comonomers, but reliable quantification of copolymerization parameters limits the development of structure-property relationships. Conventional linearization techniques to estimate comonomer reactivity ratios depend on measurements of

the partial molar conversions of each monomer at low conversions. These values can be accurately measured by NMR or GC, but such offline measurements typically provide one data point per reaction and require extensive experimental work. In situ techniques also allow rapid measurements of multiple reactions at different feed compositions.

We monitored the copolymerization of ϵ -CL and δ -valerolactone (δ -VL) using in situ Raman spectroscopy. The monomer concentration profiles are shown in Figure 3. During the first five minutes of copolymerization, the δ -VL concentration remains constant while ϵ -CL is consumed. Similar induction periods have been observed previously for δ -VL polymerized by enzyme catalysis.²⁸ The mechanistic model described earlier allowed us to identify a possible cause of the induction period. At the initial stages of copolymerization, the water present reacts with enzyme-activated monomer to form the ring-opened monomer. Although δ -VL exhibits a faster rate of hydrolysis and rate of propagation,²⁹ the ring-opened form (5-hydroxypentanoic acid) undergoes spontaneous cyclization back to the monomer faster than it can be incorporated in the growing oligomers.³⁰ The ring-opened form of ϵ -CL, 6-hydroxyhexanoic acid, undergoes lactonization at a much slower rate. Once the water present in the reaction is incorporated into the growing oligomers, around 5 minutes in this case, the δ -VL is readily incorporated in the polymer.

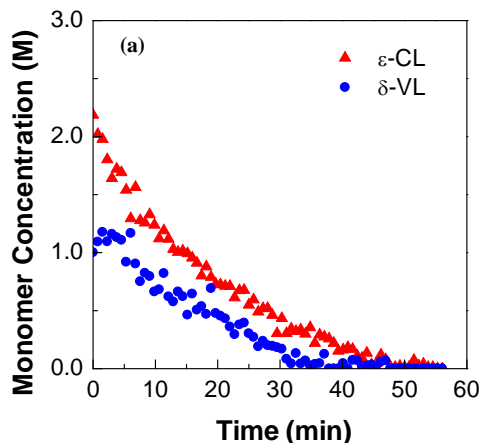


Figure 3. Monomer concentration profiles for enzymatic copolymerization of (\blacktriangle) ϵ -CL and (\bullet) δ -VL. Reproduced with permission from reference 34. Copyright 2013 The American Chemical Society.

Reactivity ratios are conventionally estimated using linearization techniques such as the Fineman-Ross and Kelen-Tüdös method (K-T method).^{31,32} We were able to use the Raman spectroscopic data to calculate the initial monomer consumption ratio, $d[\delta\text{-VL}]/d[\epsilon\text{-CL}]$, for each starting monomer ratio $[\delta\text{-VL}]/[\epsilon\text{-}$

CL]. Reactivity ratios were then determined using the K-T method as $r_{\epsilon\text{-CL}} = 0.38 \pm 0.06$ and $r_{\delta\text{-VL}} = 0.29 \pm 0.03$. These reactivity ratios indicate a slightly alternating microstructure, and are similar to ratios reported for the bulk copolymerization catalyzed by $\text{Sn}(\text{Oct})_2$ ($r_{\epsilon\text{-CL}} = 0.25$ and $r_{\delta\text{-VL}} = 0.49$).³³

Conventional reactivity ratio techniques have many problems, however. Due to the low conversion assumption, we only use a small fraction of the collected Raman data. Skeist, along with the work of Meyer and Lowry, developed a model to describe the monomer composition drift during the course of copolymerization. Applying this integrated form of the copolymer composition equation uses the spectroscopic data over the entire course of the copolymerization. Using an error-in-variables-model (EVM) nonlinear regression technique, the data was fit to the model to estimate reactivity ratios.³⁴ Figure 4 shows the spectroscopic data with model fits. The model fit the data very well, suggesting that enzyme-catalyzed copolymerizations can be effectively described by terminal model kinetics. The results from each reaction were combined to estimate the composite reactivity ratios of $r_{\epsilon\text{-CL}} = 0.27$ and $r_{\delta\text{-VL}} = 0.39$. Figure 5 shows the reactivity ratios and 95 % joint confidence regions (JCRs) from both the K-T method and the EVM method. The EVM method estimates reactivity ratios lower for $\epsilon\text{-CL}$ and higher for $\delta\text{-VL}$, which is presumably due to the lowered influence of the $\delta\text{-VL}$ induction period.

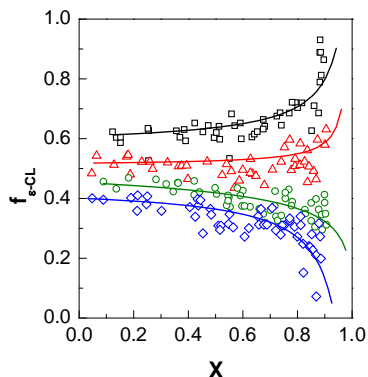


Figure 4. Monomer fraction versus total monomer conversion for enzymatic copolymerizations of $\epsilon\text{-CL}$ and $\delta\text{-VL}$. The symbols represent experimental data and the solid lines represent the best fit using EVM regression for starting compositions $f_{\epsilon\text{-CL},0}$ of (■) 0.60, (▲) 0.52, (●) 0.45, and (◆) 0.40. Reproduced with permission from reference 34. Copyright 2013 The American Chemical Society.

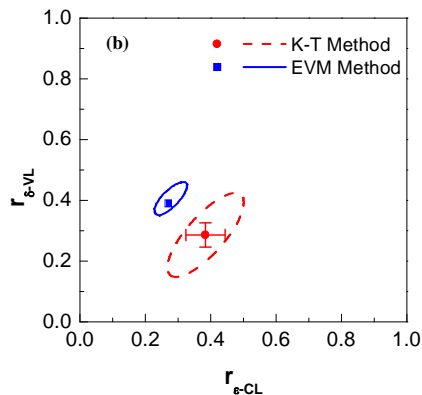
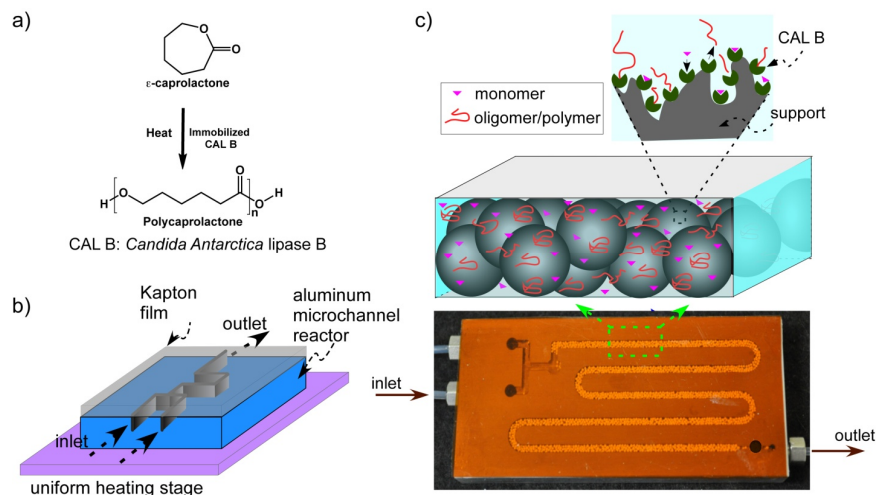


Figure 5. Reactivity ratios and 95 % JCRs for the enzymatic copolymerization of ϵ -CL and δ -VL in toluene. The error bars for the K-T method represent one standard deviation based on linear regression analysis. Reproduced with permission from reference 34. Copyright 2013 The American Chemical Society.

Engineering Control of Ring-Opening Polymerization through Microfluidic Reactor Design

Understanding the mechanism and influence of water, concentration, and temperature in enzyme catalyzed ring-opening polymerization has led to the development of packed bed microfluidic flow reactors to systematically control experimental parameters.^{9,10} The development of measurement tools to characterize enzymatic ROP must also coincide with the progress of reactor design to evaluate the advantages afforded to conducting the reaction in a microfluidic system under continuous flow. Accurate determination of process changes involving immobilized enzyme catalyst can compliment advantages of new reactor design and increase the possibilities for scaling up reactors with improved control to commercial reactor sizes.

The packed bed reactor, consisting of a 2 mm x 1 mm x 260 mm (W x D x L) channel cut into a 10 mm thick aluminum block, maintained accurate reaction temperature control to ± 0.5 °C. A depiction of the reactor design is illustrated in Scheme 3.



Scheme 3. (a) Ring-opening polymerization of ϵ -CL catalyzed by CAL B. (b) flow direction in the packed-bed microfluidic device. (c) side view of polymer chains interacting with immobilized CAL B catalyst. (4) picture of N435 packed bed microfluidic device sealed with a Kapton film (orange). Reproduced with permission from reference 9. Copyright 2011 The American Chemical Society.

ROP of ϵ -CL in the microfluidic reactor was conducted at temperatures between 55 °C – 100 °C and ϵ -CL conversion was monitored by Raman spectroscopy. The reaction reached final conversion within 240 s for all temperatures studied (Figure 6a). The rate of reaction was calculated for temperatures for the residence time in the columns and calculated from the equation below:

$$-\ln(1 - X_t) = k_{app}t$$

where X_t is the monomer conversion for residence time, t , and k_{app} is the apparent rate constant. Residence time in the reactor was controlled by flow rate. Fits of first-order reaction kinetics are shown in Figure 6b, where k_{app} values were between 0.007 s⁻¹ to 0.012 s⁻¹ for all temperatures studied. This is an order of magnitude increase for batch reactions under the same conditions, (k_{app} values between 0.0004 s⁻¹ and 0.0008 s⁻¹). This rate increase is due to the restricted volume in the packed microfluidic channel, where diffusion length to the enzyme active site is much smaller. In addition, the larger surface area to volume ratio of the microfluidic reactor relative to the batch reactor will result in more availability of enzyme active sites for faster polymerization. Active site availability and short diffusion pathways also can be attributed to the increase in M_n for the microfluidic device over batch reactors.

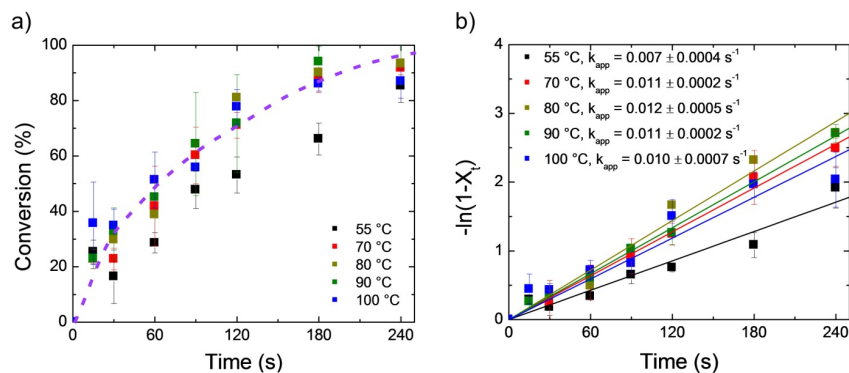


Figure 6. (a) Conversion of ϵ -CL with residence time for five temperatures. (b) Semilogarithmic conversion data fitted with first order reaction kinetics. Error bars represent one standard uncertainty of the data based on at least three measurements. Reproduced with permission from reference 9. Copyright 2011 The American Chemical Society.

The microfluidic reactor also allows for control of polymer chain ends not afforded to batch reactors. Water, which plays a critical role in lubrication and activation of the enzymes,²⁴ can also act as an initiator, forming more carboxylic acid polymer chain ends. Following on the microreactor development work, investigations into chain end control were compared between batch and microfluidic devices, monitoring reaction conversion by ^1H NMR.¹⁰ Benzyl alcohol initiator was added to batch and microfluidic reactors that were anhydrous (water from solvent and monomer removed) and wet conditions. Initiation of benzyl alcohol was dominant in the microfluidic device, regardless of starting water concentration. The fraction of benzyl chain ends from PCL synthesized in the microfluidic device was greater than 0.98 after 90 s of reaction time. While batch reactors under dry conditions demonstrate fractions of benzyl end groups similar to the microfluidic system, the mass fraction of initiated benzyl alcohol in wet conditions leads to greater carboxylic acid chain ends and benzyl alcohol fraction of less than 0.2. Tailored initiators can therefore be introduced into microfluidic reactors under less stringent conditions to incorporate endgroup functionalized polyesters for further postpolymerization reactions.

The determination of enzyme activity and stability in microfluidic devices over batch reactions is critical to process development, where improving catalyst reusability can make heterogeneous catalysts more amenable to commercial-scale polymerizations. Previously, enzyme activity over several reuse cycles in the microfluidic device has been controlled by the hydration of the active enzyme site. Rinsing the device with anhydrous toluene caused a dramatic

decrease in polymer conversion in subsequent cycles, while a “wet wash” rehydrated the enzymes and kept conversion high at 80 %.

Summary and Outlook

A wide-ranging measurement toolbox has been applied to improving understanding of enzyme-catalyzed ring-opening polymerization reactions through measuring the reaction at multiple tiers, from experimentally-validated theoretical reaction models, to on-line reaction monitoring of entire reaction mixtures. Predictive kinetic models detailing the reaction pathways of a propagating chain provide a comprehensive view of the reaction mechanism, which is supported by experimental data. Stability of the enzyme catalyst/solid support interface was measured through 2D experimental models to probe the effects of reaction conditions on catalyst retention. On-line measurement of the bulk ROP reaction mixture using Raman spectroscopy provides kinetic information without disturbing the reaction mixture. Rapid kinetic data collection of ROP is expanded to determine reactivity ratios for lactone copolymerizations to control material properties. Development of microfluidic reactors imparts rapid polymerization rates with control of polymer endgroups that were quantified in direct comparison with traditional polymerization methods.

These characterization methods can be used to quantify reaction rates and process conditions for current advances in enzyme-catalyzed ROP, including the study of new solid-supported enzymes,³⁵ development of novel monomer and co-monomer pairs,³⁶⁻³⁸ and the synthesis of branched polymers.³⁹ This comprehensive metrology approach of prediction, simplified surface models, and on-line reaction monitoring can be used to rapidly characterize and optimize novel polymerization systems, including next-generation catalysts, monomers, and reactor systems.

References

- (1) Guillaume, S. M.; Carpentier, J.-F. *Catal. Sci. Technol.* **2012**, *2*, 898–906.
- (2) Kamber, N. E.; Jeong, W.; Waymouth, R. M.; Pratt, R. C.; Lohmeijer, B. G. G.; Hedrick, J. L. *Chem. Rev.* **2007**, *107*, 5813–5840.
- (3) Kobayashi, S. *Macromol. Rapid Commun.* **2009**, *30*, 237–266.
- (4) Yang, Y.; Yu, Y.; Zhang, Y.; Liu, C.; Shi, W.; Li, Q. *Process Biochem.* **2011**, *46*, 1900–1908.
- (5) Yu, Y.; Wu, D.; Liu, C.; Zhao, Z.; Yang, Y.; Li, Q. *Process Biochem.* **2012**, *47*, 1027–1036.

- (6) Tufvesson, P.; Lima-Ramos, J.; Nordblad, M.; Woodley, J. M. *Org. Process Res. Dev.* **2010**, *15*, 266–274.
- (7) Kumar, A.; Gross, R. A. *Biomacromolecules* **2000**, *1*, 133–138.
- (8) Mei, Y.; Kumar, A.; Gross, R. A. *Macromolecules* **2002**, *35*, 5444–5448.
- (9) Kundu, S.; Bhangale, A. S.; Wallace, W. E.; Flynn, K. M.; Guttman, C. M.; Gross, R. A.; Beers, K. L. *J. Am. Chem. Soc.* **2011**, *133*, 6006–6011.
- (10) Bhangale, A. S.; Beers, K. L.; Gross, R. A. *Macromolecules* **2012**, *45*, 7000–7008.
- (11) Kao, P.; Allara, D. L.; Tadigadapa, S. *IEEE Sens. J.* **2011**, *11*, 2723 – 2731.
- (12) Liu, S. X.; Kim, J.-T. *J. Lab. Autom.* **2009**, *14*, 213–220.
- (13) Liu, C.; Meenan, B. J. *J. Bionic Eng.* **2008**, *5*, 204–214.
- (14) Laszlo, J. A.; Evans, K. O. *J. Mol. Catal. B-Enzym.* **2007**, *48*, 84–89.
- (15) Laszlo, J. A.; Evans, K. O. *J. Mol. Catal. B-Enzym.* **2009**, *58*, 169–174.
- (16) Volden, S.; Moen, A. R.; Glomm, W. R.; Anthonson, T.; Sjöblom, J. *J. Disper. Sci. Technol.* **2009**, *30*, 865–872.
- (17) Rodahl, M.; Höök, F.; Fredriksson, C.; Keller, C. A.; Krozer, A.; Brzezinski, P.; Voinova, M.; Kasemo, B. *Faraday Discuss.* **1997**, *107*, 229–246.
- (18) Voinova, M. V.; Rodahl, M.; Jonson, M.; Kasemo, B. *Phys. Scripta* **1999**, *59*, 391–396.
- (19) Orski, S. V.; Kundu, S.; Gross, R. A.; Beers, K. L. *Biomacromolecules* [Just Accepted], DOI:10.1021/bm301557y, Published online Jan, 4, 2013.
- (20) Reviakine, I.; Johannsmann, D.; Richter, R. P. *Anal. Chem.* **2011**, *83*, 8838–8848.
- (21) Johnson, P. M.; Kundu, S.; Beers, K. L. *Biomacromolecules* **2011**, *12*, 3337–3343.
- (22) Idris, A.; Bukhari, A. *Biotechnol. Adv.* **2012**, *30*, 550–563.
- (23) Varma, I. K.; Albertsson, A.-C.; Rajkhowa, R.; Srivastava, R. K. *Prog. Polym. Sci.* **2005**, *30*, 949–981.
- (24) Dong, H.; Cao, S.-G.; Li, Z.-Q.; Han, S.-P.; You, D.-L.; Shen, J.-C. *J. Poly. Sci. A Polym. Chem.* **1999**, *37*, 1265–1275.
- (25) Bisht, K. S.; Henderson, L. A.; Gross, R. A.; Kaplan, D. L.; Swift, G. *Macromolecules* **1997**, *30*, 2705–2711.
- (26) Kundu, S.; Johnson, P. M.; Beers, K. L. *ACS Macro Lett.* **2012**, *1*, 347–351.
- (27) Hunley, M. T.; Bhangale, A. S.; Kundu, S.; Johnson, P. M.; Waters, M. S.; Gross, R. A.; Beers, K. L. *Polym. Chem.* **2012**, *3*, 314–318.
- (28) López-Luna, A.; Gallegos, J. L.; Gimeno, M.; Vivaldo-Lima, E.; Bárzana, E. *J. Molec. Cat. B-Enzym.* **2010**, *67*, 143–149.
- (29) Van der Mee, L.; Helmich, F.; De Bruijn, R.; Vekemans, J. A. J. M.; Palmans, A. R. A.; Meijer, E. W. *Macromolecules* **2006**, *39*, 5021–5027.

- (30) Wiberg, K. B.; Waldron, R. F. *J. Am. Chem. Soc.* **1991**, *113*, 7697–7705.
- (31) Fineman, M.; Ross, S. D. *J. Polym. Sci.* **1950**, *5*, 259–262.
- (32) Kelen, T.; Tüdös, F. *J. Macromol. Sci. A* **1975**, *9*, 1–27.
- (33) Storey, R. F.; Hoffman, D. C. *Makromol. Chem-M Symp.* **1991**, *42-43*, 185–193.
- (34) Hunley, M. T.; Beers, K. L. *Macromolecules* [Just Accepted], DOI: 10.1021/ma302015e. Published online Feb, 5, 2013.
- (35) Barrera-Rivera, K. A.; Flores-Carreón, A.; Martínez-Richa, A. In *Lipases and Phospholipases*; Sandoval, G., Ed.; Methods in Molecular Biology; Humana Press, 2012; Vol. 861, pp. 485–493.
- (36) Poulhès, F.; Mouysset, D.; Gil, G.; Bertrand, M. P.; Gastaldi, S. *Polymer* **2012**, *53*, 1172–1179.
- (37) Frampton, M. B.; Séguin, J. P.; Marquardt, D.; Harroun, T. A.; Zelisko, P. M. *J. Molec. Cat. B-Enzym.* **2013**, *85-86*, 149–155.
- (38) Ragupathy, L.; Ziener, U.; Dyllick-Brenzinger, R.; Von Vacano, B.; Landfester, K. *J. Molec. Cat. B-Enzym.* **2012**, *76*, 94–105.
- (39) Liu, C.; Jiang, Z.; Decatur, J.; Xie, W.; Gross, R. A. *Macromolecules* **2011**, *44*, 1471–1479.